30 MeV PROTON LINEAR ACCELERATOR WITH RFQ FOCUSING

V.A.Zenin, A.P.Maltsev, I.G.Maltsev,
V.V.Nezhegorodsev, V.B.Stepanov, V.A.Teplyakov
Institute for High Energy Physics,
142284 Protvino, Moscow Region, Russia

Abstract

The systems of the proton linac with RFQ focusing are briefly described. The experimental results and exploitation ones are presented. The total prolonged observations of the sparking frequency (< 0.2%) and break-down time ratio (< 2%) are discussed.

INTRODUCTION

The 30 MeV linac (URAL-30) is the injector for the IHEP synchrotron [1] it is the first and unique accelerator with RFQ focusing up to the output energy. The accelerator design was elaborated at IHEP. This linac was commissioned in 1977 and has been operating as the injector from 1983 up to now [1-5, 15].

I. ACCELERATOR AND ITS SYSTEMS

The application of the RFQ focussing allowed one to remove some disadvantages of the traditional Alvarez structure. The new accelerating structure with the spatial homogeneous RFQ focusing (RFQ) is realized in the described accelerator. The initial part of the accelerator (IPA) with such structure was eleborated and commisioned at IHEP in 1972. It is used instead of the cumbersome 0.7 MeV preinjector.

In some years similar IPA projects (named RFQ abroad) apeared in other countries. The application of the new accelerating structure permitted to reduce the input energy to 100 keV, to accelerate 100 mA proton beams and to obtain the transmission efficiency of about 90%. The functions of the adiabatic bunching and acceleration are combined in the IPA. It differs from a usual decision when the beam is bunched first and then accelerated.

A Spatial Homogeneous Quadrupole (SHQ) focuses all the ions indepently from the velocity and phase of the particles. Such focusing can be used in the Main Part of an Accelerator (MPA). However, the method of forming the accelerating field component using the voltage on the quadrupole electrodes does not allow one to obtain the acceptable rate of the acceleration.

When particle bunches move in the homogeneous quadrupole they efficiently interact with RF field only in places of quadrupol where the field is close to the amplitude value at the moment when the bunch is there. The parts of the quadrupole with small interaction can be removed. The quadrupole channel becomes a spatial-periodic quadrupole with the same first garmonic amplitude gradient of the quadrupole field component. The necessary longitudinal field component is formed in the places where the quadrupole is removed.

The MPA accelerating structure uses H-cavity. This cavity is cheaper and smaller than a cylindrical one. The structural scheme of the accelerator is given in Fig.1. It consists of the following systems: an ion gun (IG), IPA for 2 MeV output energy, two MPA sections for 16 and 30 MeV output energy, a debuncher, RF power supply system, beam current inductive transdusers, automated control system, regulating – blocking – signalling system and technological systems.

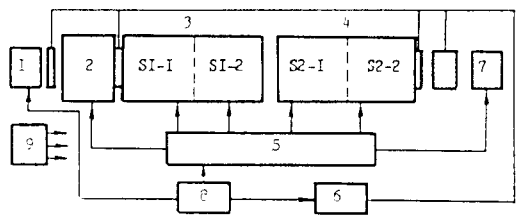

Figure 1. Structural scheme of the accelerator. 1 – ion gun with the supply system, 2 – IPA, 3,4 – MPA sections, 5 – RF power supply system, 6 – measuring system of the beam parameters, 7 – debuncher, 8 – timer system, 9 – technology system and regulating – blocking – signalling system.

The IPA electrodes are fabricated as four vanes with the edges of the sine wave profile near the beam axis. The accelerating – focusing channel has a matching section at its beginning of a funnel shape. This section decreases the acceptance dependence on the input phase of the particles. The cross-sections of the 2H-cavity and the IPA electrodes are given on Fig.2.

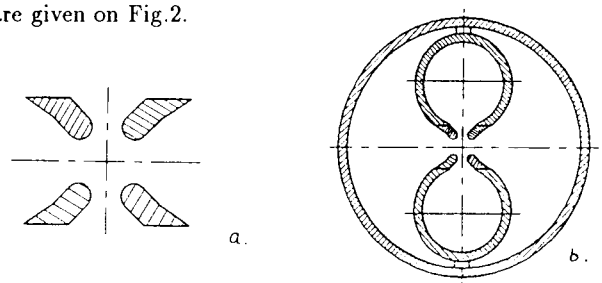

Figure 2. a – electrodes, b – 2H -cavity.

The spatial-periodic RFQ focusing is used in two MPA sections. The acceleration and focusing are realized in a "double gap" formed by three electrodes of a special shape. One of the electrodes, an "intermediate" one, is connected to the nought potential and two other are connected to the edges of the H-cavity [6-7].

The focusing field component is formed is the space between the fingers fixed on the next electrode spacers. In the first MPA section an asymmetrical structure of the double gap is used. In the first half of the double gap the fingers are withdrawn from the beam axis. They create the necessary capacity load. In the second MPA section the symmetrical double gap structure is used. In this case the fingers have the same lenghts in both halves of the double gap Fig.3. The MPA electrodes are fixed in the H-cavity, which is shown in Fig.4. The exciting mode has a longitudinal homogeneous magnetic field along the cavity. Both MPA sections are devided into two subsections (S1-1, S1-2, S2-1, S2-2) radiotechnically. It is done to obtain the fast stabilization of the field amplitude and phase in the cavity. The output proton energy is 9 MeV (for S1-1) and 23 MeV (for S2-1).

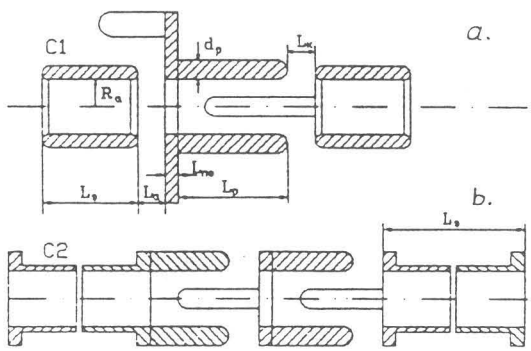

Figure 3. Accelerating MPA electrodes: a – in C1 section, b – in C2 section.

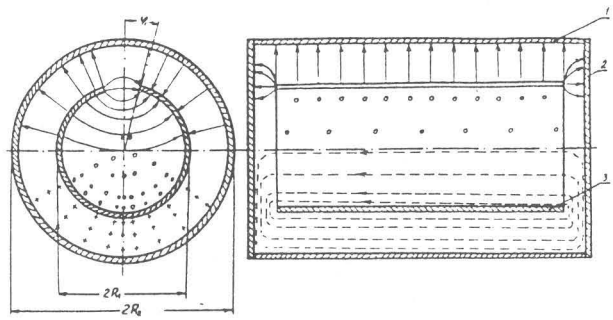

Figure 4. H– cavity. 1 – external cylinder, 2 – bottom, 3 – inner cylinder; Continuous lines are lines of the electric field, dotted lines are lines of the magnetic field.

The value of the stored energy in the H-cavity is 10-15 times smaller than in the cylindrical ones. That is why it is necessary to introduce additional power into the cavities and to create special systems of the field amplitude and phase stabilization for the ion acceleration with the 50 mA beam current and the 1 μs current pulse length and more. The RF power supply system is elaborated for the 100 mA current acceleration taking into account the necessary fast-response [9]. The RF power supply structure scheme is shown in Fig.5. The branching of the RF system is realized on the high level of the RF power. Two subsections of each section are supplied by one output RF amplifier. The RF power of the output RF amplifier enters two radiotechnical identical subsections through high-frequency bridges (HFB). The reflected wave, carrying the information about the beam load and detuning of the cavity, is extracted in the HFB shoulder decoupled from the generator. The selection method of the parameters of the generator-cavity coupling and the system of the nonlinear feed-back [10] are used in IPA.

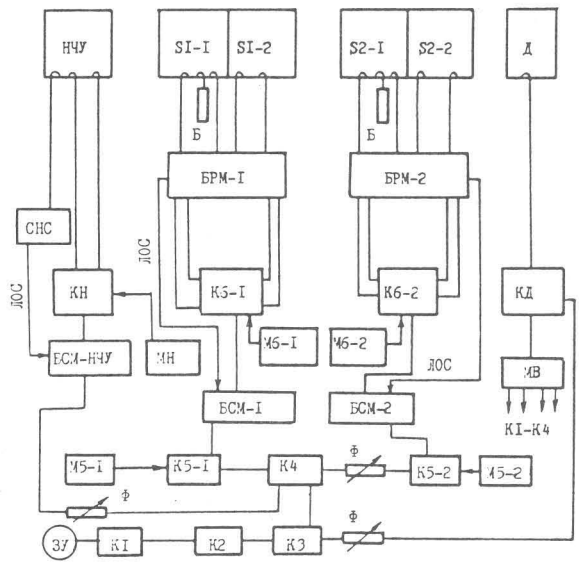

Figure 5. RF power supply structure scheme for URAL-30. IPA – initial part of the accelerater; S1-1, S1-2, S2-1, S2-2 – subsections of MPA-main part of the accelerator; D – debuncher; B – ballast load; KH, K6-1, K6-2, KD–RF power amplifiers; K1-K4, K5-1, K5-2 – intermediate RF amplifiers; MB, MH, M5-1, M5-2, M6-1, M6-2 – modulators of the anode supply system; Ф – set phase control; БРМ-1, БРМ-2 – power distribution unit; БСМ-1, БСМ-2 – power combining unit; ЛОС – feedback line; ЗУ – single-frequency signal generator; СНС – system of the nonlinear stabilization.

The ion gun with the 100 keV proton energy has a proton source with the plasma cathode [11]. The small size

of the discharge camera (1.5 cm^3) and the pulse leak-in of hydrogen maintain the ion source operation at the minimum gas flow rate. The ion gun allows one to obtain $150 \div 300$ mA current at the IPA input with 30-100 μs current pulse length. At the IPA input the pulse magnetic lens is fixed to optimize the conditions of the beam injection.

The beam parameter measuring system consists of traditional devices (the inductive transdusers, magnetic analyzer, device for measuring the emittance) and some additional devices and transdusers. In particular, the sectionalizing transdusers are used to measure the beam density distribution in the beam cross-section and the collimating mechanism is applied to study the accelerating-focusing channel by injecting collimated beams to the definite points of the cross-section of the input accelerator aperture. The measurement and analysis of the field destribution of the secondary radiation are used [12,13]. By means of the mobile and static radiation monitors the process of the cavity conditioning is controled and the estimation of the relative changes of the accelerating field distribution alonge the accelerator axis is given. At the accelerator operation with beam the places of the particle losses are defined and their dependence on different perturbations of the accelerator operation is studied. Such method allows one to tune separate accelerating sections, to define the initial and nominative levels of the RF fields, to optimize the RF field phases between the accelerating sections when the intermediate current transdusers are absent.

The electronic counters of the high-power pulses and pulse absence are fixed at the accelerator. This allows one to observe the sparking frequency in each of the sections and to make a conclusion on the stability of its operation.

The automated system permits to check the accelerator operation, to display information for an operator in a convenient form.

II. EXPERIMENTAL RESULTS AND EXPLOITATION EXPERIENCE OF INJECTOR FOR BOOSTER

The IPA and MPA peculiarities were experimentally studied when separate accelerating section were in stages.

In particular, the IPA 200 mA output current is obtained and this current is not limited. Part of the accelerated current is equal to 90% of the current, that has passed through the accelerating – focusing channel. The transmission efficiency of the longitudinal motion is about 100%. The calculated dependences of some IPA parameters at the beam acceleration are given in Fig.6. In Fig.7 the calculated and experimental beam spectra of longitudinal momenta are shown.

The main beam parameters at the MPA outputs of two sections (9 and 16 MeV energy) are about the calculated values. The beam losses are very considerable between the IPA and MPA. The main calculated parameters of the injector for the booster are given by the first table [14]. The experimental and calculated phase pictures of the beam are on Fig.8, and the beam energy spectrum is on Fig.9. At the 80 mA beam current the normalized beam emittance is not larger than 0.8 cm·mrad (95% of the particles). The operation energy spectrum, as a rule, is larger than the calculated value, this is connected with the insufficient compensation of the cavity field falling down caused beam loading. However, the energy spectrum satisfies the capture booster conditions at finer tuning.

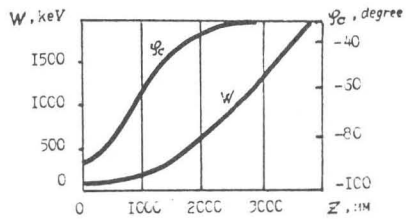

Figure 6. Dependences of the particle energy (W). and synchronous phase (φ_c) versus the length (z) for the IPA.

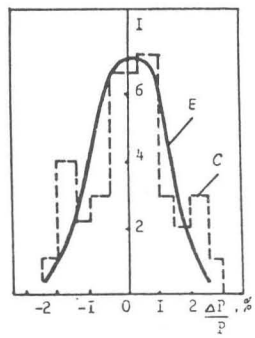

Figure 7. Distribution of the particles versus the longitudinal momentum at the IPA output. C is calculation, E is experiment, I is particle current (in per-unit), $\Delta p/p$ – momentum spread.

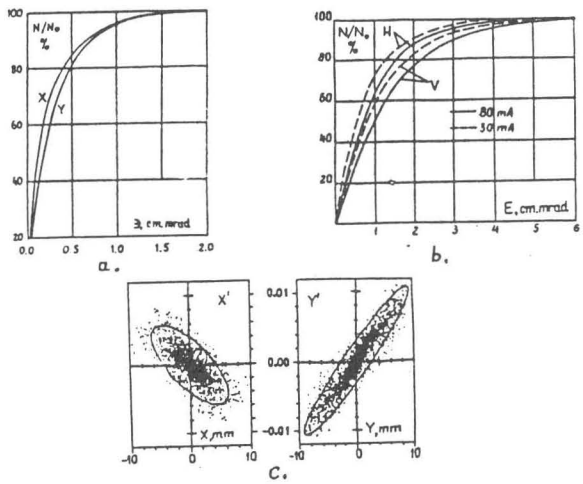

Figure 8. Particle distribution versus the emittance value. A is calculation, Э is normolized emittance, *b* is experiment, E is unnormolized emittance, c is distribution of the accelerated particles in the cross phase plane. (The measured outline for the 90% beam current is in agreement with the experiment).

Table 1.

	Parameter, notation, unit symbol	Value		
		IPA	MPA	
			1 section	2 section
1	Input energy, W_{inp} MeV	0.1	1.980	16.001
2	Output energy, W_{outp}, MeV	1.98	16.001	29.991
3	Designed proton current, J, mA	100	100	100
4	Current pulse length, τ_p, μs	10	10	10
5	Pulse repetition frecuency, f_p, Hz	25	25	25
6	Cycle repetition frequency, f_c, Hz	0.2	0.2	0.2
7	Cavity voltage, U, kV	150	304	352
8	Operating frequency, f, MHz	148,5	148,5	148,5
9	Peak surface field, E_{max}, kV/cm	225	380	370
10	Longitudinal momentum spectrum $\Delta p/p$, %	±1.5	±0.47	±0.42
11	Phase width, $\Delta\varphi$, grad	45	20	12
12	Synchronous phase, φ_c, grad	-90÷-30	-30	-30
13	Transmission efficiency, æ, %	98	-	-
14	Acceleration efficiency, ϑ	0.002÷ 0.31	0.628÷0.866	0.765÷0.809
15	Frequency of small longitudinal oscillations in the unit symbols of RF field frequency, Ω/ω	0.021÷0.092	0.086÷0.037	0.037÷0.028
16	Number of acceleration periods, N_a	136	65	57
17	Phase change of transverse oscillations of the synchrotrons particle on the focusing period, μ	0.92	1.51÷1.38	1.35
18	Minimum frequency of transverse oscillations of the synchronous particle (in t/T_{Bq}), ν_{min}	0.57	0.648÷0.709	0.687÷0.693
19	Maximum frequency of transverse oscillations of the synchrotronous particle (in t/T_{Bq}), ν_{max}	1.4	2.6÷3.2	2.6÷2.7
20	Normolized accelptance, A, mrad.cm	1.12π	0.85π	-
21	Normolized emittance for the 90% beam current, 0.1 mr.cm input beam emittance and 100 mA beam current, E, mrad·cm	0.175π	0.260π	0.326π

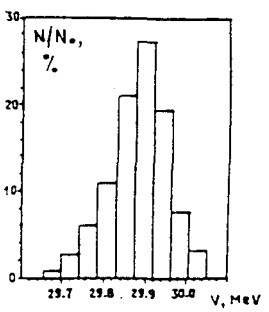

Figure 9. Energy spectrum of the accelerated particles is calculated.

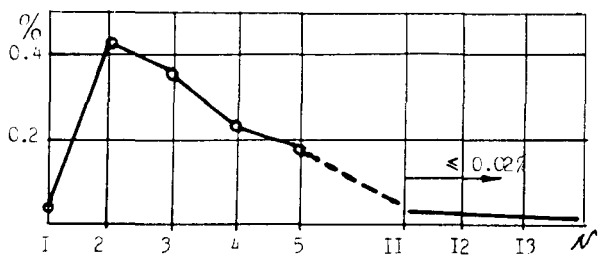

Figure 10. Change of the sparking frequency (%) in the first MPA section is given for 10 runs (each 45 days long). N=1,2,3... is a number of run N 1 correspondes to the section commissioning.

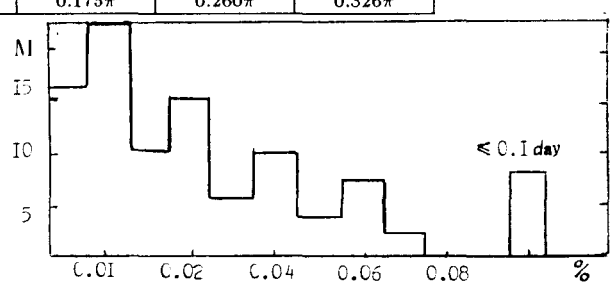

Figure 11. Number of the days (M) with the definite sparking frequency (%) is shown for the first MPA section operated during a month run (the day is equal to 8 hours).

The effective operation of the accelerating structures with RF focusing is possible at high field strength on the electrode surface. This strength was chosen to be equal to 230 kV/cm in the IPA and to 380 kV/cm in the MPA sections 2-3 times exceeds Kilpatric's value.

Long observations of the break-dowm voltages in the accelerating sections under the operation conditions show the reliable operation of these sections at the above-mentioned field strength without special conditions of fabrication and assembling. For example, the change of the sparking frequency in the first MPA section is given for 10 runs (each 45 days long) in Fig.10. The beginning of this curve corresponds to the end assembling of the new electrode. The

same dependences are recieved for other sections. In accordance with the experimental and exploitation data the sparking frequency is minimum at the new electrode assembly, then it increases because of frequent openings and assembly new sections and then it decreases and becomes stable. In Fig.11 number of the days with the definite sparking frequence is shown for the first MPA section operated during month run (the day is equal to 8 hours). As a rule, the mean sparking frequence of 5 sections is not larger than 0.1%. It is interesting to mark the equality of the sparking frequences for the IPA and MPA when the MPA field strength is 2 times large than the IPA field strength.

The experimental study of the sparking frequence allows one to make some conclusions:

- There are different films, micro pores and other dusts leading to the increase of the local electron emission that play the main part at the voltage break down the mean field strength.
- Eeach accelerating structure is characterized by its sparking frequency defined by all the totalities of the constractive and technology peculiarities, therefore it is very difficult to compare different accelerating structures by the value of the field strength.
- In a many gap system (in the accelerating channel) the break-downs are of probable character: under the same conditions the sparking frequency can change in a wide region. Therefore, there are many doubts when the data, obtained for a single vacuum gap, must be used for an accelerating structure. The reliable data can be obtained by the long-term observations of the break-downs under the operation conditions.

The accelerator with RFQ focussing has already been operating for more than 10 years as the injector for the booster of the IHEP synchrotron ensuring the physics experiments. Usually there are 5 runs per a year. In the last years the break-down time ratio was smaller than 2% that is quite well for the proton accelerators. The portion of the break-down time ratio for the accelerating structure is smaller than 10% from 2%. The basic break-down time is connected with the rafusuls of the following systems: the RF power supply system, ion gun, technological systems. In the new accelerating structure there are no difficulties with multipactoring at feeding the RF power into the cavity. The operation level of the RF field can be obtained during some hours after vacuum pumping in any accelerator section.

III. CONCLUSION

The comparison of the accelerator using the RFQ focusing and H-cavity with the accelerator using the cylindrical cavity and drift tubes with electromagnetic quadrupole lenses shows the nearness of their main parameters. However the new accelerator has advantages: the small size cavities, the low injection energy, small weight, comparatively low cost, comfortable service (exploitation). Such accelerator does not require any large building, the same 10 MeV accelerator can be placed in usual laboratory conditions. This accelerator is distinguished by the simplicity of the accelerating – focusing channel construction from the construction of the drift tubes with electromagnetic or permanent magnet quadrupoles. But there are essential disadvantages in the above-mentioned H-cavity construction of the URAL-30. The RF voltages of the accelerating period electrodes are equal along an accelerating section. Therefore the rate of the acceleration decreases with the increase of the ion velocity, the electrode voltage is limited by the break-down. The electrode capacity per meter long (H-cavity load) is about constant. The decreasing rate of the acceleration and the constant electrode capacity per meter decrease the shunt inpedance of the H-cavity. That is why the RF power in the walls of the URAL-30 sections is larger than in a similar Alwarez accelerator. There are reasons to hope that mentioned disadvantages will be removed in the new designed 60 MeV proton linac with the RFQ focussing (URAL-60) which is eleborated by IHEP.

The storing experience of the URAL-30 explotation is used to design the URAL-60 – a new injector for UNK.

Authors of this report are very grateful to all IHEP colleagues, who took part in the creation and exploitation of the URAL-30.

IV. REFERENCES

[1] V.A.Teplyakov. Preprint ITEP 10-260 Moscow (1970).
[2] V.A.Teplyakov. Prib. Tekh. Eksp. N 6 (1964). 24.
[3] I.M.Kapchinskiy, V.A.Teplyakov. Prib. Tekh. Eksp. N 2 (1940), 19.
[4] S.A.Il'evskiy et al. Atmnaya Energiya. Vol. 34(1) (1973), 56.
[5] A.A.Egorov et al. Journal of Technical Physics. Vol. 51(8), (1981), 1643.
[6] V.B.Stepanov, V.A.Teplyakov. Bulleten Izobreteniy N 14, (1968), 45.
[7] V.B.Stepanov, V.A.Teplyakov. Preprint IHEP 74-130, Serpukhov, (1974).
[8] A.P.Maltsev et al. Atomnaya Energija. Vol. 23(3) (1967), 195.
[9] I.G.Maltsev. Preprint IHEP 80-4, Serpukhov, (1980).
[10] S.P.Kuznetsov et al. Preprint IHEP 86-192 Serpukhov (1986).
[11] V.V.Nezhegorodsev. Bulleten Izobreteniy N 27 (1975), 178.
[12] V.A.Zenin, M.N.Chimankov. Preprint IHEP 85-103 Serpukhov (1985).
[13] V.A.Zenin, M.N.Chimankov. Preprint IHEP 87-36, Serpukhov (1987).
[14] A.V.Zherebtsov et al. Preprint IHEP 90-29, Protvino, (1990).
[15] V.A.Zenin et al. Procedings of the XIII International Conference on Accelerators of High Energy Charge Particles. Novosibirsk. Vol. 1, (1986), 312.